The battle against antimicrobial resistant bacterial infections: next stage development of antimicrobial peptides

Gent, M.E. van

2

C-terminal PEGylation improves SAAP-148 peptide's immunomodulatory properties

Miriam E. van Gent, Bep Schonkeren-Ravensbergen, Asma Achkif, Daan Beentjes, Natasja Dolezal, Krista E. van Meijgaarden, Jan Wouter Drijfhout and Peter H. Nibbering

Submitted

Abstract

Synthetic antibacterial and anti-biofilm peptide (SAAP)-148 was developed to combat bacterial infections not effectively treatable with current antibiotics. SAAP-148 is highly effective against antimicrobial resistant (AMR) bacteria without inducing resistance, however challenges for further development of SAAP-148 include its cytotoxicity and short circulation half-life. To circumvent these drawbacks a library of SAAP-148 linked to polyethylene glycol (PEG) groups of various lengths was synthesized and screened for *in vitro* antibacterial activity and hemolytic activity. Results indicated that PEGylated SAAP-148 variants combine antibacterial activities with reduced hemolysis compared to SAAP-148. Interestingly, pro-inflammatory immunomodulatory activities of SAAP-148 were enhanced upon C-terminal PEGylation, with SAAP-148-PEG_{27} showing most effect. SAAP-148-PEG_{27} enhanced SAAP-148's capacity to chemoattract human neutrophils and was able to more efficiently (re)direct M-CSF-induced monocyte-macrophage differentiation towards type 1 macrophages as opposed to SAAP-148. Furthermore, dendritic cells with a stronger mature expression profile were produced if monocytes were exposed to SAAP-148-PEG_{27} during monocyte-immature dendritic cell differentiation in comparison to SAAP-148. Parameters that influenced the immunomodulatory activities of the peptide-PEG conjugate include i) the length of the PEG group, ii) the position of PEG conjugation, and iii) the peptide sequence. Together, these results indicate that SAAP-148-PEG_{27} is highly effective in redirecting monocyte-macrophage differentiation towards a proinflammatory phenotype and promoting monocyte-mature dendritic cells development. Therefore, SAAP-148-PEG_{27} may be a promising agent to modulate inadequate immune responses in case of tumors and chronically infected wounds.

1. Introduction

Host defense peptides (HDPs) are a class of small peptides that span 10-60 amino acids in length, of which most contain a prominent cationic net charge at physiological pH [1]. HDPs have shown to exhibit a diverse set of biological activities, including antimicrobial and immunomodulatory activities, for instance reduction of proinflammatory cytokine production, modulation of chemokine expression and alteration of macrophage and leukocyte differentiation [2-4]. The best studied human HDP is LL-37, a member of the cathelicidin family, that serves as first-line defense as part of the human innate immunity. This amphipathic helical peptide is expressed as prepropeptide hCAP-18 [5] which after extracellular processing by proteolytic enzymes yields LL-37, and has shown moderate, broad-spectrum antimicrobial activity against planktonic and biofilm-residing bacteria [6, 7]. The ability of LL-37 and other amphipathic HDPs to adopt an alfa-helix near the bacterial membrane is critical for their antimicrobial activity [8, 9]. LL-37 has also been well-studied for its prominent immunomodulatory activities, including wound healing [10]. LL-37 was shown to chemoattract immune effector cells [11] and is capable of modulating cytokine and chemokine expression by a range of cells [12]. Furthermore, LL-37 can (re)direct macrophage differentiation towards a pro-inflammatory subset of macrophages [13]. Moreover, LL-37 was also identified as potent modifier of DC differentiation, up-regulating endocytosis and expression of costimulatory molecules, enhancing cytokines and overall promoting Th-1 responses *in vitro* [14]. Interestingly, exposure of phytohemagglutinin-activated peripheral blood mononuclear cells (PBMCs) to LL-37 resulted in higher T-cell proliferation, promoted Treg generation and decreased expression of proinflammatory factors compared to activated PBMCs [15]. Overall, LL-37 exhibits a diverse set of activities that can modulate aspects of both innate and adaptive immunity.

To increase the antimicrobial activity of LL-37, we developed a range of synthetic derivatives of this peptide, including synthetic antimicrobial and antibiofilm peptide (SAAP)-148. This peptide has shown excellent antimicrobial activity against multidrug-resistant bacteria *in vitro* and was able to completely eradicate biofilm-associated infections with methicillin-resistant *Staphylococcus aureus* (MRSA) and *Acinetobacter baumannii* from murine skin [16]. Additionally, SAAP-148 was very effective in eradication of MRSA persisters generated inside mature biofilms [17]. However, immunomodulatory activities of SAAP-148 have not been investigated. Challenges for further development of SAAP-148 include its relative cytotoxicity and short circulation half-life. Therefore, chemical modification of SAAP-148 by covalent attachment of polyethylene glycol (PEG) polymer chains, i.e. PEGylation, was considered as strategy to circumvent these drawbacks.

PEGylation of HDPs with sufficiently long PEG-chains (>2000 kDa) has been associated with decreased hemolytic and cytotoxic activities, increased peptide stability by protection against proteolytic enzymes, reduced serum protein binding and improved solubility [18-22]. However, these advantages come with the cost of reduced antimicrobial activity ranging from 2-fold up to 64-fold or even total loss of activity depending on the HDP used. Reduced antimicrobial activity of HDPs upon PEGylation has been positively correlated with increasing PEG-lengths [22, 23]. Thus, coupling of HDPs to shorter low molecular weight PEG-chains may reduce their cytotoxicity and improve their circulation half-life, while minimizing reduction of their antimicrobial activity. For instance, Cui et al. showed that OM19r-8 PEGylated at the N-terminus with PEG5 resulted in improved proteolytic stability, reduced hemolytic activity and prolonged half-life in rat, while slightly reducing antimicrobial activity by 2.5-fold [24]. Additionally, Morris et al. reported that PEG_2-CaLL and PEG_3-CaLL minimally decreased antimicrobial activity by 2-fold to 3-fold, while improving cytotoxicity *in vitro* and lung tissue biocompatibility in rat *ex vivo* [25]. Three critical parameters that may influence the characteristics of PEGylated HDPs include the size of the PEG group, the site of covalent attachment of the PEG group and the type of linker used [23].

Based on considerations above, we hypothesized that attachment of low molecular weight PEG groups to termini of SAAP-148 does not affect the peptide's antibacterial activities, while reducing its cytotoxic actions and modulating SAAP-148 immune regulating activities. To test this hypothesis, a library of SAAP-148 peptides linked at the N- or C-terminal site to low molecular weight PEG groups of various lengths was synthesized and screened for hemolytic activities and antimicrobial activities against planktonic *S. aureus* and *Escherichia coli* and biofilm-residing *A. baumannii*. Based on previous findings that LL-37 skews the immune landscape to a pro-inflammatory response, we investigated the ability of the PEGylated SAAP-148 peptides to affect a variety of innate immune responses, including human neutrophil migration, human macrophage differentiation and dendritic cell maturation.

2. Materials and methods

2.1. Peptide synthesis

Peptides were synthesized by Fmoc chemistry on an automated multiple peptide synthesizer (Syro II, MultiSyntech, Witten, Germany) and PEG chains were coupled as Fmoc amino acid. Peptides synthesized for this study include SAAP-148, LL-37, CMV-1 and derivatives thereof with PEG substitutions of different lengths attached to the C-terminus or N-terminus of the peptide. The sequences of these peptides can be found in **Table 1**. The purity of the peptides was >95% (except for PEG_{11} variants

that had purity of 72-86%), as determined by reverse-phase high performance liquid chromatography (HPLC) and mass spectrometry confirmed the molecular mass of the peptides. Afterwards, the peptides were lyophilized and stored at -20 °C until use. Peptides were dissolved in Milli-Q to a stock of 5.12 mM, aliquoted and stored at -20 °C. Prior to the experiments, the peptide-stocks were further diluted into the medium of choice and used directly.

2.2. Bacteria

In this study the following antimicrobial resistant (AMR) strains were used: *A. baumannii* strain RUH875; *S. aureus* strain LUH14960 (JAR) and methicillin-resistant *S. aureus* (MRSA) LUH14616 (NCCB100829); and *E. coli* strain LUH15108 and colistin-resistant *E. coli* strain LUH15117. Bacteria were stored in glycerol at -80 °C until use. Prior to experiments, bacteria were cultured overnight on blood agar plates at 37 °C. Then, bacteria were cultured to mid-log phase in tryptic soy broth (TSB) for 2.5 h at 37 °C while rotating at 200 rpm. Afterwards, bacteria were centrifuged at 1,000 g for 10 min, washed once and resuspended in the preferred medium to the required concentrations based on the optical density at 600 nm.

2.3. *In vitro* killing assay

Mid-log phase bacteria were resuspended in PBS to a concentration of 5 x 10^6 CFU/mL. Thereafter, 20 µL of bacterial suspension was mixed with 30 µL of PBS containing

Table 1. Set of PEGylated SAAP-148, LL-37 or CMV-1 peptides used in this study.

Peptide name	Sequence	MW (g/mol)
SAAP-148	Acetyl – L K R V W K R V F K L L K R Y W R Q L K K P V R – amide	3269.6
SAAP-148-PEG_2	Acetyl – L K R V W K R V F K L L K R Y W R Q L K K P V R – PEG_2 – amide	3471.2
SAAP-148-PEG_3	Acetyl – L K R V W K R V F K L L K R Y W R Q L K K P V R – PEG_3 – amide	3516.4
SAAP-148-PEG_5	Acetyl – L K R V W K R V F K L L K R Y W R Q L K K P V R – PEG_5 – amide	3605.2
SAAP-148-PEG_{11}	Acetyl – L K R V W K R V F K L L K R Y W R Q L K K P V R – PEG_{11} – amide	3866.8
SAAP-148-PEG_{27}	Acetyl – L K R V W K R V F K L L K R Y W R Q L K K P V R – PEG_{27} – amide	4572.5
Y-PEG_{27}	Y – PEG_{27} – amide	1484.8
PEG_{11}-SAAP-148	PEG_{11} – L K R V W K R V F K L L K R Y W R Q L K K P V R – amide	3825.6
PEG_{27}-SAAP-148	PEG_{27} – L K R V W K R V F K L L K R Y W R Q L K K P V R – amide	4531.0
LL-37	L L G D F F R K S K E K I G K E F K R I V Q R I K D F L R N L V P R T E S	4493.3
LL-37-PEG_{27}	L L G D F F R K S K E K I G K E F K R I V Q R I K D F L R N L V P R T E S – PEG_{27} – amide	5796.9
scLL-37	L G F R S E I K F R V R K F R L P T S L D F K K K G E K I Q I D L N V R E	4493.3
scLL-37-PEG_{27}	L G F R S E I K F R V R K F R L P T S L D F K K K G E K I Q I D L N V R E – PEG_{27} – amide	5796.9
CMV-1	G P Q Y S E H P T F S Q Y R I – amide	1810.0
CMV-1-PEG_{27}	G P Q Y S E H P T F S Q Y R I – PEG_{27} – amide	3113.5

Acronyms: SAAP-148 = synthetic antibacterial and anti-biofilm peptide 148; PEG_n = polyethylene glycol with chemical structure $C_{2n+5}H_{4n+9}O_{n+2}$; sc = scrambled; CMV-1 = cytomegalovirus peptide 1; MW = molecular weight. One-letter-coding was used for amino acids.

increasing concentrations of peptide and 50 µL of filtered, heat-inactivated pooled human plasma (Sanquin, Leiden), pooled human urine (healthy human volunteers) or PBS in polypropylene V-shaped 96-wells microplates (Greiner BioOne, Germany). After 2 h incubation at 37 °C under rotation at 200 rpm, 10-fold serial dilutions were plated onto Mueller-Hinton (MH) plates to determine the number of viable bacteria. Results are expressed as lethal concentration $(LC)_{99.9}$, i.e. the lowest concentration of peptide that killed 99.9% of the inoculum.

2.4. Anti-biofilm assay

Mid-log phase bacteria were diluted to 1 x 10^7 CFU/mL in BHI (Brain Heart Infusion broth, Oxoid), 100 µL of bacterial suspension was added to each well of a polypropylene flat bottom microplate (Greiner BioOne, Germany) and incubated for 24 h at 37 °C in humidified environment. Afterwards the biofilms were washed twice with PBS to remove remaining planktonic bacteria and the biofilms were exposed to increasing peptide concentrations in PBS. The plates were sealed with non-breathable plastic film sealers (Amplistar adhesive plate sealers, Westburg) and incubated for 2 h at 37 °C under continuous shaking. Medium controls were used to monitor possible contamination. Finally, the biofilms were washed twice with PBS and bacteria were harvested in 100 µL of PBS by sonication (Branson 1800, 10 min). The number of viable bacteria was assessed microbiologically. Results are expressed as biofilm eradication concentration $(BEC)_{99.9}$, i.e. the lowest concentration of peptide that killed 99.9% of the biofilm-encased bacteria.

2.5. Hemolysis assay

Human erythrocytes were isolated from fresh blood of anonymized healthy donors obtained after written informed consent (LUMC Blood Donor Service, LuVDS, Leiden, the Netherlands). Fresh blood was collected in citrate tubes, centrifuged at 3,000 rpm to pellet the erythrocytes, washed three times with PBS and diluted to a 2% erythrocyte suspension in PBS. Subsequently, 25 µL of PBS containing a titration series of the peptides were mixed with 50 µL of pooled human plasma and 25 µL of 2% human erythrocytes in wells of a polypropylene V-shaped microplate (Greiner BioOne, Germany). A 5% (v/v) Triton-X solution in demineralized water and PBS were included as positive and negative controls, respectively. The plate was incubated for 1 h at 37 °C and 5% CO_2 after which the erythrocytes were pelleted by centrifugation for 3 min at 1,200 rpm. The supernatant was transferred to a 96-wells flat-bottom plate and the optical density was measured at 415 nm. Results are expressed as percentage hemolysis relative to the controls:

$$\text{Hemolysis (\%)} = \frac{\text{OD415}_{\text{sample}} - \text{OD415}_{\text{negative control}}}{\text{OD415}_{\text{positive control}} - \text{OD415}_{\text{negative control}}} \times 100\% \quad (1)$$

2.6. Chemotaxis of human neutrophils

Human neutrophils were isolated from fresh blood of anonymized healthy donors obtained after written informed consent (LUMC Blood Donor Service, LuVDS, Leiden, the Netherlands) using Ficoll amidotrizoate (ρ=1.077 g/mL, department of Clinical Pharmacy and Toxicology, Leiden University Medical Center, Leiden, the Netherlands) density gradient centrifugation at 700 x g for 20 min. Erythrocytes in the pellet were lysed using lysis buffer comprising 0.1 mM EDTA (Sigma, St. Louis, MO, USA), 180 mM NH_4Cl (Merck, Darmstadt, Germany) and 10 mM $KHCO_3$ (Merck, Darmstadt, Germany) dissolved in ultrapure water and remaining neutrophils were washed twice with PBS and resuspended in RPMI medium 1640 (Gibco Life Technologies, Bleiswijk, the Netherlands). Transwell filters (pore size 3.0 µm, Greiner BioOne, #665631) were preincubated with 0.1% (w/v) bovine serum albumin (BSA; Fraction V, Roche) in PBS to prevent binding of the cells to the filter. Next, 3-4 x 10^5 neutrophils suspended in RPMI medium were pipetted on top of each transwell, and increasing peptide concentrations in RPMI medium below the transwell filters as chemoattractant. Positive and negative controls were 10 nM N-formyl-methionyl-leucyl-phenylalanine (fMLP, Sigma) in RPMI medium spiked with 10% (w/v) heat inactivated fetal bovine serum (FBSi, Corning) and RMPI medium, respectively. Neutrophils were incubated for 90 min at 37 °C and 5% CO_2 after which 5 mM ethylenediaminetetraacetic acid (EDTA, Sigma Life Science, St. Louis, USA) was added to the lower compartment to harvest adherent cells. Next, cell counts of neutrophils in the lower compartment were performed on a BD Accuri C6 flow cytometer (Becton Dickinson). Results are expressed as percentage of neutrophils migrated compared to the positive control fMLP, which was set at 100%.

2.7. Effect of peptide on monocyte-macrophage differentiation

Peripheral blood mononuclear cells (PBMCs) were isolated from anonymized healthy donor buffy coats obtained after written informed consent (Sanquin Blood Bank, Leiden, the Netherlands) using Ficoll amidotrizoate density gradient centrifugation (ρ=1.077 g/mL). Monocytes were further purified by selecting for $CD14^+$ cells using anti-CD14-conjugated magnetic microbeads (Miltenyi Biotec) according to manufacturer's protocol. As described earlier by Verreck et al. [26], macrophages type 1 (Mφ-1) and 2 (Mφ-2) were produced in 12 wells culture plates (Greiner BioOne) by culturing 1 x 10^6 monocytes per well with GM-CSF and M-CSF, respectively. Briefly, monocytes were cultured for 7 days in RPMI medium 1640 containing 10% (w/v) FBSi, 1% (w/v) pen/strep [2 mM penicillin, 2 mM streptomycin (Gibco Life Technologies)] and 1% glutamax [2 mM L-glutamine (Gibco Invitrogen)] and 10 ng/mL GM-CSF (Milteny Biotec) or 50 ng/mL M-CSF (Bio-Techne, Minneapolis, MN, US) further referred to as culture medium. Culture medium was refreshed at day 3 and the cells were exposed to LPS (Sigma) at day 6 and at day 7 the cell-surface

marker expression and cytokine profile were assessed.

To study the effect of (PEGylated) SAAP-148 on M-CSF-driven monocyte-Mφ differentiation, monocytes were additionally exposed to peptide (up to 3.2 μM) at day 0 of the culture compared to the culture medium. To verify differentiation of monocytes into Mφ-1 or Mφ-2, the Mφs were observed at day 6 of the culture using microscopy (Olympus TL4). Afterwards, the cells were stimulated overnight with 100 ng/mL LPS (LD Sigma) and expression of cell-surface receptors was assessed using PE-conjugated monoclonal antibodies (mAbs) directed against CD11b (clone ICRF44, BD pharmingen), FITC-conjugated mAbs directed against CD14 (clone M5E2, BD pharmingen) and alexafluor700-conjugated mAbs directed against CD163 (clone RM3/1, Biolegend). Mφs were stained with these mAbs in 0.1% (w/v) BSA in cold PBS for 30 min. Finally, samples were measured on a BD Accuri C6 using flow cytometry and analyzed with BD Accuri C6 software version 1.0.264.21. Additionally, supernatants of Mφ cultures were collected for assessment of the production of cytokines IL-10 and IL-12p40 using commercially available enzyme-linked immunosorbent assay (ELISA) kits (Biolegend) according to manufacturer's instructions. Lower limits of detection in these ELISAs were 15.6 and 62.5 pg/mL for IL-10 and IL-12p40, respectively.

2.8. Effect of peptide on Mφ-2 redirection towards Mφ-1

Mφ-2 generated in 7 days as described above were exposed to peptide (up to 3.2 μM) or as control to the M-CSF-containing culture medium. After 3 days culture medium was refreshed for medium containing M-CSF but not peptide. Three days thereafter Mφs were checked microscopically and afterwards stimulated with LPS. The next day the Mφs were harvested and expression of cell-surface markers and production of cytokines by the cells was assessed as described above.

2.9. Effect of peptide on monocyte-immature dendritic cell differentiation

Monocytes were isolated as described above. Immature dendritic cells (iDCs) were produced in 12 wells culture plates by culturing 1 x 10^6 monocytes per well for 7 days in culture medium containing 10 ng/mL GM-CSF and 10 ng/mL IL-4 (Bio-Techne) [14]. Culture medium was refreshed at day 3.

To study the effect of (PEGylated) SAAP-148 on monocyte-iDC differentiation, monocytes were additionally exposed to peptide (up to 3.2 μM) at day 0 of the culture compared to the culture medium containing GM-CSF and IL-4. On day 6 immature dendritic cells were harvested and expression of cell-surface receptors of these iDCs was assessed using FITC-conjugated mAbs directed against CD14 (clone M5E2, BD pharmingen), PE-conjugated mAbs directed against CD11b (clone ICRF44,

BD pharmingen), alexafluor700-conjugated mAbs directed against CD1a (clone H1149, Biolegend), PE-conjugated mAbs directed against CD209 (clone DCS-8C1, Biolegend), APC-conjugated mAbs directed against CD40 (5C3, BD pharmingen), PE-conjugated mAbs directed against CD83 (clone HB15e, BD pharmingen), PE-conjugated mAbs directed against CD80 (clone L307.4, BD Biosciences), FITC-conjugated mAbs directed against CD86 (clone 2331 (FUN-1), BD pharmingen) and FITC-conjugated mAbs directed against HLA-DR (clone G46-6, BD pharmingen). iDCs were incubated with these mAbs and the samples were acquired and analyzed using flow cytometry (BD Accuri C6 using BD Accuri C6 software).

2.10. Effect of peptide on antigen processing and presentation by iDCs

The antigen processing and presentation capabilities of (PEGylated) SAAP-148-induced and control iDCs were studied using T cell proliferation as read-out [27]. Presentation of peptide 3-13 from *M. tuberculosis* HSP65 was assessed by coculturing $2.5x10^3$ HLA-DR3 matched monocyte-derived peptide-exposed iDCs with 10^4 T cells from an established T cell clone (Rp15 1-1) specific for peptide 3-13. As assay control $5x10^4$ irradiated (2,000 rad) HLA-DR3 matched PBMC's were cocultured with the T cell clone and its cognate peptide. Cells were cultured in IMDM supplemented with Glutamax, 1% (w/v) pen/strep and 10% pooled human serum (Merck, Darmstadt, Germany) in presence of 1-10 µg/mL peptide 3-13 for a total of 72 h at 37 °C and 5% CO_2. Antigen processing and presentation of purified protein derivative of *M.tuberculosis* (PPD) was assessed using the same set-up as above (concentration range 1 – 10 µg/ml). After 72 h supernatants were harvested for further analysis of IFN-γ production using ELISA (U-CyTech biosciences, Utrecht, the Netherlands). Data is represented as median and individual values from at least three experiments performed in triplicate.

2.11. Secondary structural conformation of peptide

Circular dichroism spectroscopy was performed at room temperature using a Jasco J-815 CD spectrometer with a 1 mm path-length cell and a bandwidth of 2.0 nm. SAAP-148 and SAAP-148-PEG_{27} were prepared in 10 mM sodium phosphate (NaPi) buffer (pH 7.4) with a final peptide concentration of 0.2 mg/mL. Further analysis was performed by addition of 25% 2,2,2-trifluoroethanol (TFE; α-helix enhancer) or 1-10 mM sodium dodecyl sulfate (SDS; β-sheet enhancer or α-helix enhancer at non-micellar and micellar concentration, respectively). Spectra were recorded from 190 to 260 nm at an interval of 0.1 nm. Each spectrum was the average of five scans and blank subtraction. Secondary structure composition differences were calculated using the software CDNN 2.1 (Developed by Applied Photophysics Ltd).

2.11. Statistics

Kruskal Wallace test was used to evaluate possible differences in functional activities of SAAP-148 with low molecular weight PEG groups of various lengths attached to the C or N terminus. Differences between more groups were further evaluated by a Mann-Whitney rank sum test or Wilcoxon test for paired samples using Graphpad Prism software version 6.0 (Graph Pad Software, San Diego, CA, US). Differences were considered statistically significant when $P<0.05$.

3. Results

3.1. C-terminal PEGylation of SAAP-148 improves its antibacterial selectivity index

A set of C- and N-terminal PEGylated SAAP-148 peptides (**Table 1**) was compared to determine the effect of PEGylation with PEG groups of increasing length on antibacterial and cytotoxic activities of SAAP-148. We first compared the antibacterial activity of SAAP-148 and its C-terminal PEGylated variants against a panel of planktonic (AMR) bacterial strains. Results revealed that compared to SAAP-148 the $LC_{99.9}$ of C-terminal PEGylated SAAP-148 variants increased 4-fold at maximum against MRSA in 50% plasma (**Table 2**). Interestingly, compared to SAAP-148 the $LC_{99.9}$ was lowered up to 4-fold for C-terminal PEGylated variants of SAAP-148 against *E. coli* in 50% urine. In addition, results for 24 h biofilm residing *Acinetobacter baumannii* revealed that SAAP-148-PEG_{27} eradicated the biofilm at a concentration

Table 2. Hemolytic and antibacterial activities and resulting selectivity index of SAAP-148 and PEGylated SAAP-148 variants.

	IC_{50} (μM)	$LC_{99.9}$ (μM)	S.I.	$LC_{99.9}$ (μM)	S.I.
	Human erythrocytes	MRSA (LUH14616)	MRSA	*E. coli* (LUH15117)	*E. coli*
	50% plasma	50% plasma		50% urine	
SAAP-148	**117** (115-208)	**12.8** (6.4-12.8)	**9.2**	**12.8** (6.4-25.6)	**9.2**
SAAP-148-PEG_2	**252** (246-258)	**12.8** (12.8-25.6)*	**19.7**	**3.2******	**78.7**
SAAP-148-PEG_3	**263** (259-500)*	**12.8** (12.8-25.6)*	**20.6**	**3.2** (3.2-6.4)***	**82.3**
SAAP-148-PEG_5	**272** (236-291)*	**25.6** (12.8-25.6)**	**10.6**	**3.2** (1.6-6.4)***	**85.0**
SAAP-148-PEG_{11}	**292** (269-332)*	**25.6** (25.6-51.2)****	**11.4**	**6.4** (3.2-6.4)***	**45.6**
SAAP-148-PEG_{27}	**322** (312-597)*	**51.2** (51.2-102.4)****	**6.3**	**6.4** (6.4-25.6)	**50.3**
Y-PEG_{27}	**≥409.6**	**≥204.8**	**-**	**≥51.2**	**-**
PEG_{27}-SAAP-148	**192** (159-214)	**51.2******	**3.8**	**12.8** (6.4-12.8)	**15.0**

Hemolysis of human erythrocytes in 50% human plasma is expressed as IC_{50}, i.e the estimated concentration to induce 50% hemolysis after 1 h exposure to (PEGylated) SAAP-148. Results are shown as median (and ranges) of 2-5 independent experiments performed in triplicate. The bactericidal activity of (PEGylated) SAAP-148 upon 2 h incubation with planktonic bacteria in PBS, 50% plasma or 50% urine is expressed as $LC_{99.9}$, i.e. the lowest concentration killing 99.9% of the planktonic bacteria. Results are shown as median (and ranges) of at least three independent measurements performed in duplicate. Selectivity index (S.I.) = IC_{50} / $LC_{99.9}$. Statistical differences using Mann-Whitney tests are indicated as * for $P\leq0.05$, ** for $P\leq0.01$, *** for $P\leq0.001$ and **** for $P\leq0.0001$ compared to SAAP-148.

of 25.6 μM, similar to SAAP-148 (median of three independent measurements performed in duplicate). As a control, PEG_{27} coupled to a single tyrosine did not induce bacterial killing or biofilm eradication at any of the tested concentrations. Furthermore, the introduction of PEG_{27} and the site of PEGylation (N- or C-terminus) hardly affected the bactericidal activity of SAAP-148 against multiple *S. aureus* and *E. coli* strains (**Table 3**).

Next, the hemolytic activity of these PEGylated SAAP-148 variants was assessed using human erythrocytes (**Table 2**). Results revealed that 1 h exposure of human erythrocytes to 117 μM SAAP-148 resulted in 50% hemolysis. Hemolysis of SAAP-148 was step-wise reduced (IC_{50}=252-322 μM) when conjugated at the C-terminus to PEG groups with length from 2 to 27, clearly indicating that increasing chain lengths of PEG at the C-terminus are associated with reduced hemolysis. N-terminal PEGylation with PEG_{27} only slightly reduced hemolysis (IC_{50}=192 μM), thus N-terminal coupling of PEG groups seems less favorable for reduction of SAAP-148's hemolysis. Of note, peptide concentrations up to 51.2 μM and controls up to 204.8 μM all resulted in <5% hemolysis.

The selectivity index, i.e. the ratio between hemolysis and bactericidal activity, was calculated based on the results in 50% biological fluids. C-terminal PEGylation of SAAP-148 increased the selectivity index up to 2.2-fold for MRSA and up to 9.2-fold for *E. coli*, while for N-terminal PEGylation with PEG_{27} the selectivity index was reduced with 2.4-fold for MRSA and minimally increased by 1.6-fold for *E. coli* (**Table 2**). Thus, C-terminal PEGylation was most favorable for improving the selectivity index of SAAP-148, especially against Gram-negative bacteria.

Table 3. Bactericidal activities of SAAP-148 and N-terminal and C-terminal PEGylated SAAP-148 variants.

			$LC_{99.9}$ (μM)		
Species	**Strain**	**Medium**	**SAAP-148**	**PEG_{27}-SAAP-148**	**SAAP-148-PEG_{27}**
S. aureus	LUH14960	PBS	**0.4**	**0.8**	**1.6** (0.8-1.6)
		50% plasma	**25.6** (12.8-51.2)	**25.6** (25.6-102.4)	**51.2** (25.6-102.4)
MRSA	LUH14616	50% plasma	**12.8** (6.4-12.8)	**51.2**	**51.2** (51.2-102.4)
E. coli	LUH15108	PBS	**0.4**	**0.8**	**0.8** (0.8-1.6)
		50% urine	**1.6** (1.6-3.2)	**3.2** (1.6-6.4)	**3.2** (3.2-6.4)
E. coli	LUH15117	50% urine	**12.8** (6.4-25.6)	**12.8** (6.4-12.8)	**6.4** (6.4-25.6)

The bactericidal activity in PBS, 50% plasma or 50% urine is expressed as $LC_{99.9}$, i.e. the lowest concentration killing 99.9% of the bacteria, where the values are shown as median (and range) of at least three independent measurements performed in duplicate.

3.2. Enhanced chemotaxis of human neutrophils by C-terminal PEG_{27}-modified SAAP-148 and LL-37 but not control peptide

Next, to investigate the ability of a selection of PEGylated peptides to modulate the immune system we first compared the activity of C-terminal PEGylated SAAP-148 variants to trigger neutrophils at concentrations up to 1.6 μM as higher concentrations of SAAP-148, i.e. 3.2 μM, were cytotoxic for the neutrophils. Results revealed that the ability of SAAP-148 to trigger migration of human neutrophils was greatly enhanced by C-terminal coupling to PEG chains with increasing length from 5 to 11 to 27 units (**Figure 1a**). SAAP-148-PEG_{27} most effectively triggered neutrophil migration. In contrast, this was not observed for increasing the PEG chain length attached to the N-terminus of SAAP-148. Additionally, PEG_{27} coupling to the C-terminus of LL-37 also resulted in enhanced migration of human neutrophils (**Figure 1b**). This was less pronounced for PEG_{27} coupling to scrambled LL-37 (scLL-37) and not observed for coupling to control peptide CMV-1, indicating that peptide sequence and intrinsic chemotactic properties of the peptide are crucial for enhanced neutrophil migration upon PEGylation. As expected, the Y-PEG_{27} control did not induce migration of neutrophils (**Figure 1b**). Also, the combination of the separate components SAAP-148 and Y-PEG_{27} did not enhance migration of neutrophils compared to SAAP-148, indicating that the PEG_{27} group has to be coupled to SAAP-148 for improved activity. Together, the length of the PEG group, the position where the PEG group is attached to the peptide and the sequence of the peptide are all exclusively important for the enhanced chemotactic ability of PEGylated cathelicidins SAAP-148 and LL-37.

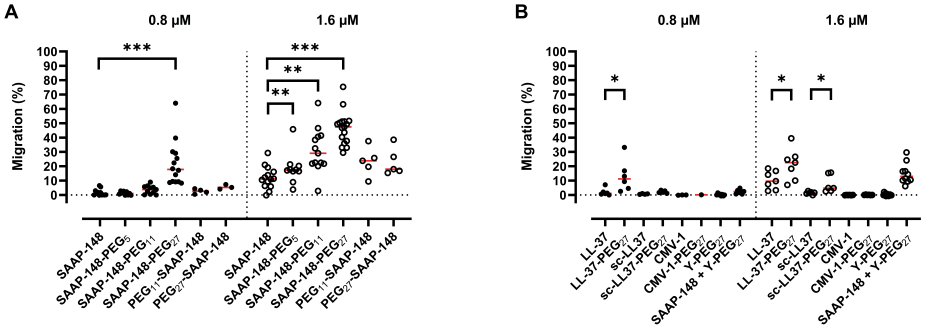

Figure 1. Chemotaxis of human neutrophils in response to SAAP-148, LL-37 and control peptide CMV-1 and PEGylated versions thereof. (a) Migration of human neutrophils in response to 0.8 or 1.6 μM of C-terminal and N-terminal PEGylated SAAP-148 peptides. (b) Comparison of migration by SAAP-148, LL-37 and CMV-1 and C-terminal PEG_{27} variants. Results are shown as percentage of neutrophils migrated compared to the positive control 10 nM fMLP, which was set at 100%. Results are expressed as median values of 4-17 independent experiments. Statistical differences between two groups are depicted as * for P≤0.05, ** for P≤0.01 and *** for P≤0.001 as calculated using Wilcoxon's paired t-test.

3.3. (Re)direction of macrophages type-2 towards type-1 by C-terminal PEG_{27}-modified SAAP-148

As cathelicidins like LL-37 affect *in vitro* monocyte-Mφ differentiation [13], we next compared the ability of SAAP-148 and SAAP-148-PEG_{27} to (re)direct monocyte-Mφ differentiation. The experimental set-up used is depicted in **Figure 2a** (**i**) and monocytes were differentiated with M-CSF and GM-CSF respectively to pro-inflammatory Mφ-1 and anti-inflammatory Mφ-2 and distinguished based on morphology (**ii, iii**), cell-surface marker expression and cytokine production: Mφ-1 are defined by classical "fried egg" morphology, $CD163^{low}$ expression, $IL\text{-}10^{low}$ and $IL\text{-}12^{high}$ production, while Mφ-2 are defined by stretched spindles, $CD163^{high}$ expression, $IL\text{-}10^{high}$ and $IL\text{-}12^{low}$ production [28]. Results revealed that culturing monocytes in presence of M-CSF and SAAP-148 (**iv**) changed the morphology of the resulting Mφs from spindles to predominantly "fried egg" cells, and more importantly for SAAP-148-PEG_{27} exposure, all Mφs developed "fried egg" morphology (**v**) whereas Y-PEG_{27} by itself did not show any changes on morphology (**vi**). In addition, SAAP-148-directed Mφs expressed reduced levels of CD163 compared to Mφ-1 (**Figure 2b**). Strikingly, culturing monocytes in presence of both M-CSF and SAAP-148-PEG_{27} led to Mφs completely lacking CD163 expression levels, indicating monocyte-Mφ differentiation was directed to a more pro-inflammatory phenotype (Mφ-1-like subset) by SAAP-148-PEG_{27}. These observations were further supported by increased CD11b and decreased CD14 expression levels (significant differences with $P=0.0159$ and $P<0.0001$, respectively, see **Table 4**) and cytokine profile, i.e. diminished IL-10 and enhanced IL-12p40 production of the resulting Mφs (**Figure 2c,d**). In addition, we found that fully differentiated Mφ-2 could be redirected towards Mφ-1-like subset by culturing Mφ-2 in presence of the conjugated SAAP-148-PEG_{27} but not SAAP-148 or Y-PEG_{27} (**Figure 2e-g** and **Table 5**). Thus, SAAP-148-PEG_{27} directs monocytes-Mφ differentiation to a pro-inflammatory Mφ-1-like subset and is able to redirect differentiated anti-inflammatory Mφ-2 to a pro-inflammatory Mφ-1-like subset.

Table 4. Cell surface marker expression of monocyte-derived Mφs and effect of addition of 1.6 μM SAAP-148, SAAP-148-PEG_{27}, Y-PEG_{27} or combination of SAAP-148 and Y-PEG_{27} on cell surface marker expression levels.

	M-CSF (Mφ-2)	+ SAAP-148	+ SAAP-148-PEG_{27}	+ Y-PEG_{27}	+ SAAP-148 + Y-PEG_{27}	GM-CSF (Mφ-1)
CD11b	**64,353** (63,192-90,272)	**110,491** (94,085-197,671)	**159,621** (73,082-161,632)	**67,821** (54,674-86,003)	**144,781** (81,602-207,960)	**148,979** (94,279-187,164)
CD14	**110,514** (97,302-155,331)	**93,393** (72,944-102,250)	**59,685** (58,930-69,405)	**102,713** (86,548-149,410)	**78,057** (60,655-95,459)	**63,351** (44,087-109,829)
CD163	**49,210** (14,286-508,236)	**10,268** (7,355-466,462)	**5,342** (4,824-45,318)	**38,492** (14,032-410,505)	**10,276** (7,778-445,104)	**5,104** (5,012-12,240)

Mφs were stained with specific monoclonal antibodies and analyzed by flow cytometry. Indicated are the median (and ranges) of the mean fluorescence intensity (MFI) of three independent experiments (CD11b and CD14b were only measured twice for the combination of SAAP-148 and Y-PEG_{27}).

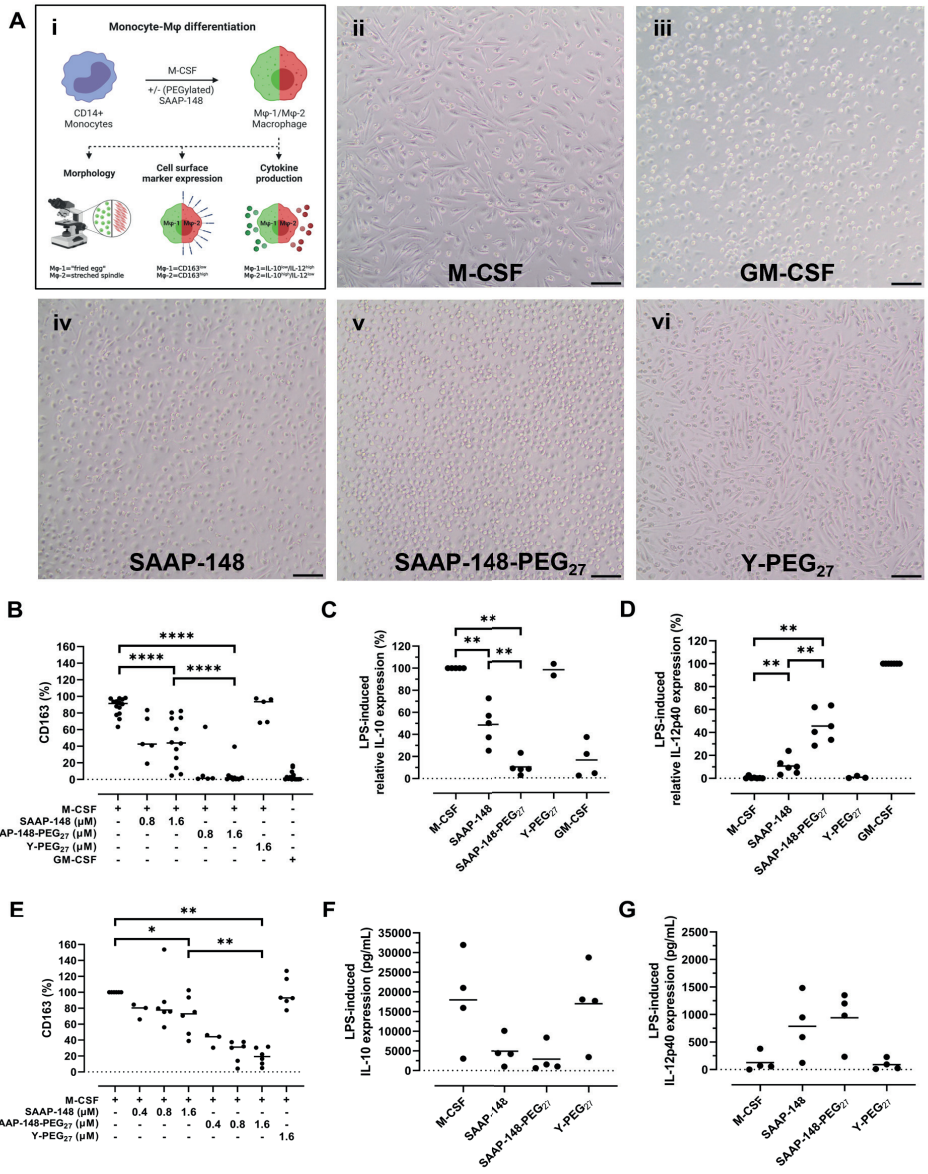

Table 5. Cell surface marker expression of Mφ-2 and effect of addition of 1.6 μM SAAP-148, SAAP-148-PEG$_{27}$, Y-PEG$_{27}$ or combination of SAAP-148 and Y-PEG$_{27}$ on expression levels.

	M-CSF (Mφ-2)	+ SAAP-148	+ SAAP-148-PEG$_{27}$	+ Y-PEG$_{27}$
CD11b	**41,330** (26,969-92,218)	**55,122** (51,733-79,563)	**80,833** (67,421-118,498)	**43,221** (341,79-99,808)
CD14	**175,237** (149,638-271,575)	**163,177** (130,718-235,378)	**125,457** (64,841-194,676)	**170,832** (163,117-294,054)
CD163	**270,378** (57,244-208,424)	**99,901** (40,398-253,049)	**28,679** (17,393-46,108)	**209,297** (53,045-264,467)

Mφs were stained with specific monoclonal antibodies and analyzed by flow cytometry. Indicated are the median (and ranges) of the mean fluorescence intensity (MFI) of three independent experiments.

◄ Figure 2. Effect of SAAP-148, SAAP-148-PEG$_{27}$ and Y-PEG$_{27}$ on monocyte-Mφ differentiation using morphology, CD163 expression and IL-10 and IL-12p40 cytokine expression as read outs. (a) Describes the (i) experimental set-up of monocyte-Mφ differentiation and morphological changes of M-CSF-driven Mφ differentiation in the presence of (iv) 1.6 μM of SAAP-148, (v) SAAP-148-PEG$_{27}$ or (vi) Y-PEG$_{27}$ in comparison to results for (ii) M-CSF and (iii) GM-CSF-triggered differentiation (scale bar indicates 100 μm). Effect of SAAP-148 and its PEGylated version on the ability to (b) direct M-CSF-driven Mφ differentiation towards Mφ-1 and (e) redirect M-CSF-driven Mφ-2 towards Mφ-1 type using CD163 expression as read out. Results are expressed relative to the expression by Mφ-2 as median and individual values of 3-14 independent experiments. Of note, the control cells exposed to M-CSF for 7-days showed a small second population that did not express CD163. For direct M-CSF-driven Mφ differentiation to Mφ-1 by 1.6 μM SAAP-148, SAAP-148-PEG$_{27}$ and Y-PEG$_{27}$ cytokine expression levels were determined for (c) IL-10 and (d) IL-12p40. Results are expressed as median and individual values of 2-6 independent experiments. For direction of M-CSF-driven Mφ differentiation by 1.6 μM SAAP-148, SAAP-148-PEG$_{27}$ and Y-PEG$_{27}$ cytokine expression was determined for (d) IL-10 relative to fully differentiated Mφ-1 in presence of M-CSF (levels ranged from 1,435 to 33,907 pg/mL) and (e) IL-12p40 relative to fully differentiated Mφ-2 in presence of GM-CSF (levels ranged from 4,643 to 51,982 pg/mL). Results are expressed as median and individual values of 2-6 independent experiments. For redirection of M-CSF-driven Mφ-2 to Mφ-1 by 1.6 μM SAAP-148, SAAP-148-PEG$_{27}$ and Y-PEG$_{27}$ cytokine expression levels were determined for (f) IL-10 and (g) IL-12p40. Results are expressed as median and individual values of 4 independent experiments. Statistical differences between two groups are depicted as * for P≤0.05, ** for P≤0.01 and **** for P≤0.0001 as calculated by the Mann-Whitney U-test.

3.4. Development of immature dendritic cells in presence of C-terminal PEG$_{27}$-modified SAAP-148

In addition to their function as Mφ precursor, monocytes have the capability to differentiate into DCs through another differentiation route. The ability of SAAP-148 and SAAP-148-PEG$_{27}$ to direct in vitro monocyte-iDC differentiation was investigated by culturing purified monocytes in the presence of GM-CSF, IL-4 and increasing doses of these peptides. A summary of the cell-surface marker expression levels at most optimal peptide concentration (0.8 μM) compared to the controls is listed in **Table 6**. Results revealed that iDCs, developed in presence of 0.4-1.6 μM SAAP-148-PEG$_{27}$, expressed elevated levels of maturation markers on their surface, i.e. CD83, CD86 and HLA-DR, compared to control iDCs (**Figure 3a-c**). Expression levels of CD209 (DC-SIGN) and CD1a (marker for iDC) by iDCs generated in presence of 0.4-1.6 μM SAAP-148-PEG$_{27}$ were considerably reduced compared to control iDCs (**Figure 3d,e**). The presence of SAAP-148 did also result in iDCs with upregulated expression of maturation markers, but this effect was less pronounced than for SAAP-148-PEG$_{27}$ and was only observed at higher concentrations (0.8 and 1.6 μM). At 0.8 μM SAAP-148-PEG$_{27}$-induced iDCs produced significantly more CD83 and CD86 and less CD209 and CD1a compared to SAAP-148-induced iDCs. Addition of Y-PEG$_{27}$ during monocyte-iDC differentiation did not result in iDCs with upregulated expression of maturation markers, nor did the combination of SAAP-148 and Y-PEG$_{27}$ compared to their controls. Together, SAAP-148-PEG$_{27}$ directs monocyte-iDC differentiation to a more mature iDC subset compared to control iDCs and SAAP-148-induced iDCs.

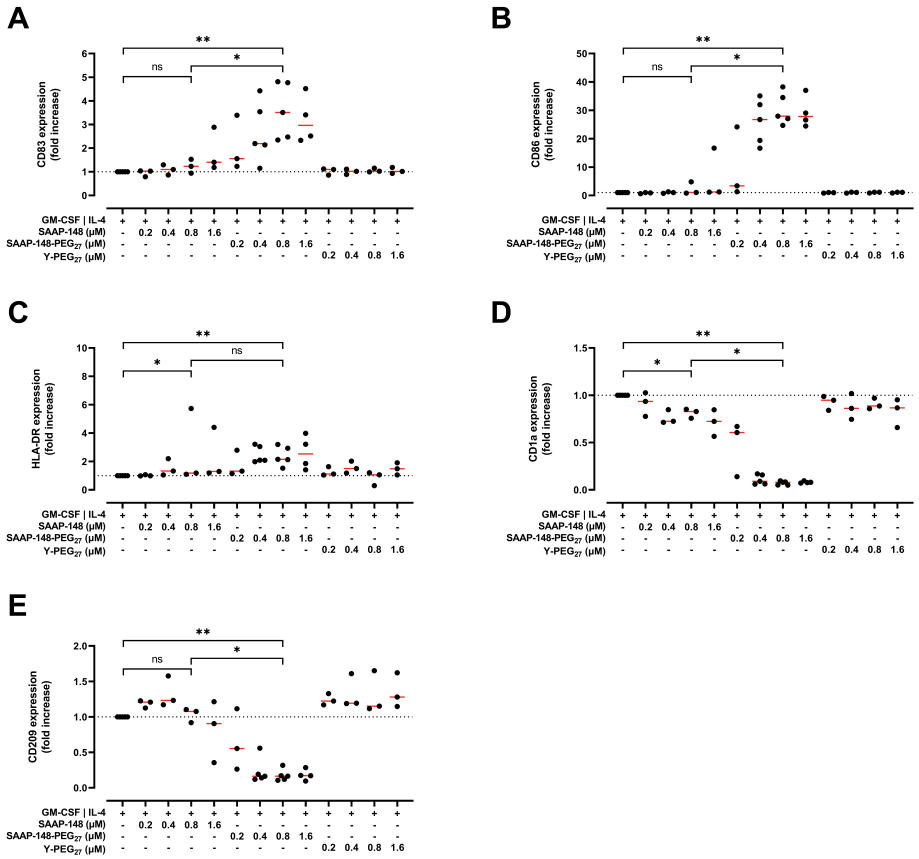

Figure 3. Effect of SAAP-148, SAAP-148-PEG$_{27}$ or Y-PEG$_{27}$ on monocyte-iDC differentiation. Effect on iDC differentiation was based on surface receptor expression of (a) CD83, (b) CD86, (c) HLA-DR, (d) CD1a and (e) CD209. Results are shown as median of at least three individual measurements expressed as fold increase of the mean fluorescence intensity (MFI) over the control. Statistical differences between two groups are depicted as ns for P>0.5, * for P≤0.05 and ** for P≤0.01 as calculated by the Mann-Whitney U-test.

3.5. Antigen processing and presentation by SAAP-148-PEG$_{27}$-induced and control iDCs is not different

Next, the ability of SAAP-148-PEG$_{27}$-induced and control iDCs to process and present antigens was assessed using clonal T cells specific for *M. tuberculosis* peptide 3-13 of hsp65. Results revealed that iDCs developed in the presence of SAAP-148-PEG$_{27}$ equally well presented peptide 3-13 to T cells and were as effective in the antigen processing of PPD compared to control iDCs (**Figure 4a,b**). These results indicate that although SAAP-148-PEG$_{27}$-induced iDCs express higher levels of maturation markers, their capacity to process and present antigens is not enhanced compared to control iDCs.

Table 6. Cell surface marker expression of monocyte-derived iDCs and effect of addition of 0.8 μM SAAP-148, SAAP-148-PEG$_{27}$, Y-PEG$_{27}$ or combination of SAAP-148 and Y-PEG$_{27}$ on expression levels.

	GM-CSF|IL-4 (iDC)	+ SAAP-148	+ SAAP-148-PEG$_{27}$	+ Y-PEG$_{27}$	+ SAAP-148 + Y-PEG$_{27}$
CD14	**8,571** (7,065-11,131)	**8,083** (7,988-13,171)	**9,262** (6,907-11,733)	**9,529** (7,916-13,304)	**9,121** (8,675-11,125)
CD11b	**84,369** (75,196-93,542)	**132,642** (105,555-159,730)	**114,241** (74,961-153,521)	**101,066** (98,364-103,768)	**91,623** (74,961-108,285)
CD1a	**41,875** (35,781-52,461)	**31,676** (30,493-43,411)	**3,982** (1,812-4,350)	**35,923** (31,708-50,856)	**37,694** (36,086-43,589)
CD209	**228,775** (207,464-252,860)	**229,167** (210,101-272,342)	**37,470** (26,723-65,636)	**290,955** (231,539-377,675)	**201,948** (176,433-233,144)
CD40	**1,085** (730-1,307)	**1,177** (1,015-1,263)	**1,462** (1,197-1,498)	**911** (742-1,399)	**1,376** (981-1,621)
CD83	**1,460** (1,379-1,962)	**2,105** (1,375-2,416)	**4,852** (3,425-6,575)	**1,453** (1,413-2,263)	**1,969** (1,532-2,044)
CD80	**5,555** (3,136-5,597)	**5,030** (3,518-6,232)	**2,723** (2,424-5,768)	**5,344** (5,033-6,126)	**4,760** (3,065-6,194)
CD86	**6,195** (5,798-9,020)	**9,339** (4,843-29,763)	**213,692** (143,145-252,120)	**7,083** (4,955-10,267)	**7,906** (6,334-18,384)
HLA-DR	**55,744** (34,900-67,401)	**79,392** (61,029-200,019)	**111,647** (102,805-163,123)	**59,193** (10,299-81,216)	**78,199** (66,999-97,049)

iDCs were stained with specific monoclonal antibodies and analyzed by flow cytometry. Indicated are the median (and ranges) of the mean fluorescence intensity (MFI) of three independent experiments (CD11b was measured in two experiments).

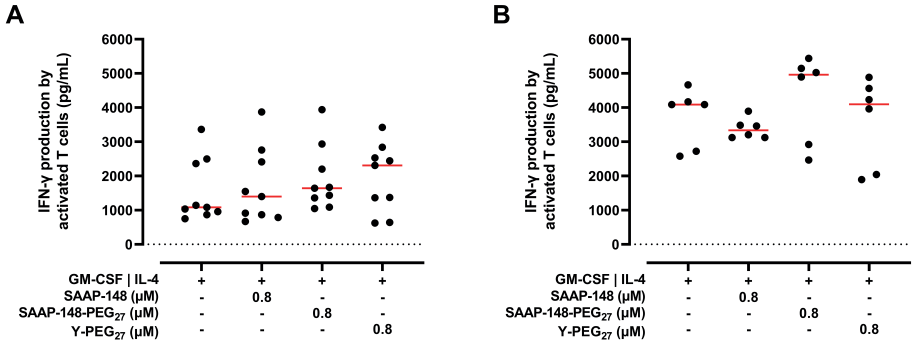

Figure 4. Antigen processing and presentation by (PEGylated) SAAP-148-induced iDCs. IFN-γ production by Th1 cell clones was used as read-out for iDC antigen presentation of (a) 1 μg/mL peptide 3-13 and antigen processing and presentation of (b) 10 μg/mL purified protein derivative (PPD). Results are shown as median of at least three experiments performed in quadruplicate that were pooled before IFN-γ measurement.

3.6. C-terminal PEG$_{27}$-modified SAAP-148 adopts different secondary structure in membrane-mimicking environment compared to SAAP-148

The ability of amphipathic HDPs, like SAAP-148 and LL-37, to structure into a compact amphipathic α-helix near the cell membrane is strongly correlated to their antimicrobial activity [9]. Structural differences upon PEGylation of SAAP-148 could play a role in the improved pro-inflammatory immunomodulatory activities of neutrophils, Mφs and iDCs upon exposure to SAAP-148-PEG$_{27}$. Therefore, we compared the conformational structures of SAAP-148 and SAAP-148-PEG$_{27}$ in buffer at physiological pH and with the addition of structure stabilizers TFE and SDS. Results showed that both peptides were unstructured at physiological pH and adopted an α-helical conformation when exposed to buffer containing 25% TFE

(**Figure 5a,b**), known to stabilize α-helical conformations in peptides and proteins [29]. Interestingly, SAAP-148-PEG_{27} was conformed into a predominantly α-helical structure (helical content = 92.8%) in contrast to SAAP-148 that partly precipitated and formed mostly anti-parallel beta-sheets (helical content = 5.2%) in presence of 1 mM SDS (**Figure 5c**), known to stabilize beta-sheets at these quasi-micellar concentrations [30, 31]. SAAP-148 completely redissolved at micellar concentrations of SDS (10 mM), where SDS acts as α-helix enhancer and both peptides adopted an α-helical conformation. These results suggest that the PEG_{27}-group promotes the α-helical content and solubility of SAAP-148 in the quasi-micellar environment induced by SDS.

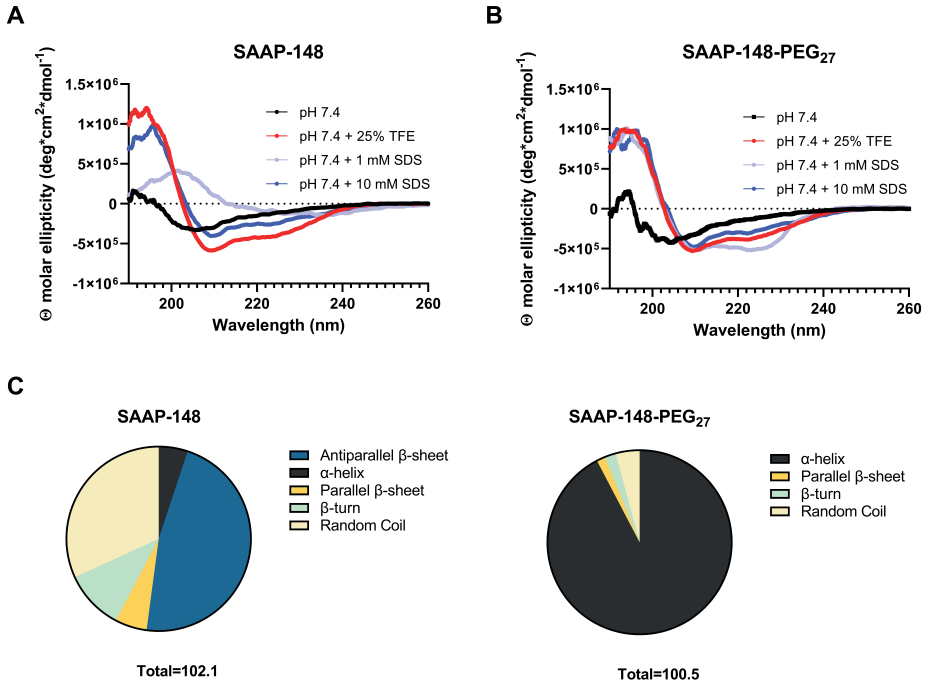

Figure 5. Secondary structural conformation of SAAP-148 and SAAP-148-PEG_{27} at physiological pH and with addition of TFE or SDS. Secondary structures of (a) SAAP-148 and (b) SAAP-148-PEG_{27} were determined in 10 mM sodium phosphate buffer (pH 7.4) with the addition of 25% trifluoroethanol (TFE) or 1-10 mM sodium dodecyl sulphate (SDS) using circular dichroism. (c) The secondary structure composition differences between SAAP-148 and SAAP-148-PEG_{27} in sodium phosphate buffer with addition of 1 mM SDS.

4. Discussion

Here we report that C-terminal PEGylation of SAAP-148 enhanced pro-inflammatory/immunomodulatory activities of this HDP towards cells involved in innate immunity, i.e. neutrophils, macrophages, dendritic cells. To our knowledge, this is the first time that enhanced immunomodulatory activities of an HDP upon PEGylation with a low

molecular weight PEG is reported. The enhanced pro-inflammatory activities of innate immune cells upon exposure to SAAP-148-PEG_{27} could be of great importance in diseases, like tumors and chronic wound infections, where it is beneficial to skew the anti-inflammatory immune landscape to a pro-inflammatory environment. Our observation that SAAP-148-PEG_{27}, in contrast to SAAP-148, easily adopts an α-helical structure may (partly) explain the enhanced immunomodulatory activities of SAAP-148-PEG_{27}.

Structure-activity relationship studies with PEGylated HDPs using neutrophil migration as read-out provided us with important insights regarding essential molecular features underlying the improved immunomodulatory activities of SAAP-148. First, increasing the PEG length from 5 repeating units to 27 increased the ability of SAAP-148 to dose-dependently chemoattract human neutrophils. Second, C-terminal attachment of PEG to SAAP-148 was superior over N-terminal attachment for promoting immunomodulatory activities. Likewise, conjugation site preferences have been observed for other ligands depending on the active site of the peptide [32, 33]. Third, PEG_{27} has to be coupled to HDPs with intrinsic chemotactic properties, like SAAP-148 or LL-37, to promote chemotaxis, as attachment to a non-HDP or scrambled HDP did not induce neutrophil chemotaxis. Fourth, PEG_{27} is only able to enhance intrinsic immunomodulatory activities of the HDP when directly conjugated, because Y-PEG_{27} or mixing Y-PEG_{27} with SAAP-148 did not exert enhanced chemotaxis of human neutrophils. Thus, the length of the PEG group, the position where the PEG group is conjugated to the HDP and the sequence of the HDP all contribute to the enhanced immunomodulatory activities.

As SAAP-148 is a synthetic derivative of LL-37, we hypothesized that both peptides potentially have a similar mechanism of action. It is known that LL-37 utilizes formyl-peptide receptors to chemoattract neutrophils [11, 34]. SAAP-148 was able to chemoattract human neutrophils to the same extend as LL-37 and C-terminal PEGylation enhanced this capability for both HDPs. Potentially, SAAP-148 and PEGylated versions of SAAP-148 utilize the same receptor as LL-37. Van der Does et al. showed that LL-37 has to be internalized by monocytes to skew M-CSF-driven Mφ differentiation from anti-inflammatory Mφ-2 to pro-inflammatory Mφ-1 [13]. Therefore, we speculate that SAAP-148 similarly needs to be internalized by endocytosis and/or via a receptor-mediated pathway. However, at present nothing is known about the cellular uptake of SAAP-148 or PEGylated peptides like SAAP-148-PEG_{27}. Moreover, Tomasinsig et al. demonstrated that LL-37 required a strong helix-forming propensity to induce cellular growth by activation of the P2X7 receptor [35]. Conformational studies with SAAP-148 and SAAP-148-PEG_{27} did reveal structural differences between SAAP-148 and SAAP-148-PEG_{27} upon

addition of 1 mM SDS. SAAP-148 precipitated and formed beta-sheets, although it should be noted that SAAP-148 redissolved at higher SDS concentrations, an effect that has been recognized for other cationic molecules in combination with SDS [36]. Thus, solubility and helix-formation of SAAP-148 is hampered at quasi-micellar concentrations of SDS. Generally, PEGylation of peptides and proteins improves their solubility [37] . Indeed, SAAP-148-PEG_{27} did not precipitate and was predominantly conformed in an α-helical structure in contrast to SAAP-148. PEGylation thus prevented precipitation, improved SAAP-148's solubility and induced an α-helical conformation in the SDS-induced quasi-micellar environment.

Furthermore, the present study shows that C-terminal PEGylation of SAAP-148 with low molecular weight PEG groups enhanced the selectivity index of this peptide towards Gram-positive and Gram-negative bacteria based on the findings that i) antimicrobial activity is improved up to 2.2-fold or 9.2-fold, for planktonic MRSA and *E. coli*, respectively, and anti-biofilm activity to *A. baumannii* immature biofilms is maintained and ii) cytotoxicity is reduced up to 2.7-fold towards human erythrocytes. These findings are in agreement with previous observations that conjugation of low molecular weight PEG chains to HDPs minimally reduces bactericidal activity, while decreasing cytotoxicity against human erythrocytes and human primary lung epithelial cells [24, 25, 38]. Hence, SAAP-148-PEG_{27} combines optimal immunomodulatory activities with improved solubility and reduced cytotoxicity, while conjugation to the low molecular weight PEG group allows SAAP-148 to reach the bacterial target regardless.

SAAP-148-PEG_{27} could be a valuable agent for treatment of diseases where it is beneficial to skew the anti-inflammatory immune response to a more pro-inflammatory one. An example comprises persistent pathogens that upon infection can suppress immune responses by promoting an anti-inflammatory immune landscape that allows the pathogen to survive and persist at its location, e.g. in chronic wounds or infected implant materials [39]. Anti-inflammatory Mφ-2 have been shown to inhibit pro-inflammatory immune responses in context of (myco) bacterial stimulation and Mφ-2 to Mφ-1 polarization can skew the host response to pro-inflammatory immune responses thereby clearing infections [26, 28]. In the present study, SAAP-148-PEG_{27} efficiently skewed monocytes and anti-inflammatory Mφ-2 to a more pro-inflammatory Mφ-1-like subset and thus has potential to restore inadequate development and pro-inflammatory activities of Mφs in persistent infections. Another example where the most abundant Mφ subset is polarized to an anti-inflammatory Mφ-2-like subset, comprises the microenvironment of tumors [40]. These tumor-associated macrophages (TAMs) with a Mφ-2d phenotype of Mφ-2s, suppress the immune system by production of anti-inflammatory cytokines, e.g.

IL-10 and TGF-β, and promote tumor initiation, growth, development and metastasis [41]. In agreement with observations of Etzerodt et al., we hypothesize that local targeting of $CD163^{high}$ TAMs will lift this immune suppression resulting in infiltration of activated T cells into the tumor and ultimately in tumor regression [42]. Initial experiments in our lab indicated that culturing monocytes in presence of 50% tumor conditioned medium resulted in $CD163^{high}$ Mφs, while 0.8 μM SAAP-148-PEG_{27} redirected this monocyte-Mφ differentiation to the more beneficiary $CD163^{low}$ pro-inflammatory Mφ-1-like subset ($p=0.049$ using unpaired t-test). This data illustrates the possibility that TAMs can be redirected to pro-inflammatory Mφ-1 by local administration of SAAP-148-PEG_{27}. This could be a promising strategy to treat solid tumors that comprise large numbers of TAMs. Obviously, possible redirection of TAMs by SAAP-148-PEG_{27} in tumor-bearing mice and its effects on tumor size should be investigated.

Together, this study shows that SAAP-148-PEG_{27} is an effective antibacterial agent with reduced cytotoxic activities and improved solubility that is able to skew an anti-inflammatory immune landscape to a pro-inflammatory environment. SAAP-148-PEG_{27} therefore holds promise as agent to (re)direct inadequate anti-inflammatory immune responses, e.g. in tumors and chronically infected wounds.

Author contributions

Conceptualization, M.E.v.G., J.W.D. and P.H.N. ; methodology, M.E.v.G., K.E.v.M., J.W.D. and P.H.N.; validation, M.E.v.G, B.S. and N.D.; formal analysis, M.E.v.G., B.S. and N.D.; investigation, M.E.v.G., B.S., A.A., D.B., N.D. and K.E.v.M.; resources, K.E.v.M., J.W.D. and P.H.N.; writing-original draft preparation, M.E.v.G. and P.H.N.; writing-reviewing and editing, M.E.v.G and P.H.N.; visualization, M.E.v.G.; supervision, P.H.N.; project administration: P.H.N.; funding acquisition, P.H.N. All authors have read and agreed to the published version of the manuscript.

Funding

This research was funded by the Dutch Research Council (NWO), Novel Antibacterial Compounds and Therapies Antagonizing Resistance Program: grant number 16434.

Statement of Ethics

For this study we used fresh human blood (LUMC Blood Donor Service, LuVDS) and buffy coats (Sanquin Blood Bank), both from anonymized healthy donors after obtaining written informed consent. The study protocols were reviewed and approved by the LUMC Biobank Review Committee (approval number LuVDS23.010) and the Sanquin Ethical Advisory Board (approval number NVTO128.02), respectively. Human cells were isolated from whole blood and buffy coats according to article 467

of the Dutch Law on Medical Treatment Agreement and the Code for Use of Human Tissue of the Dutch Federation of Biomedical Scientific Societies. The Declaration of Helsinki principles were followed when working with human cells.

Data availability statement

All data generated or analyzed during this study are included in this article. Further enquiries can be directed to the corresponding author.

Conflicts of interest

The authors have no conflicts of interest to declare.

References

1. Huan Y, Kong Q, Mou H, Yi H. Antimicrobial Peptides: Classification, Design, Application and Research Progress in Multiple Fields. Front Microbiol. 2020;11:582779.
2. Hilchie AL, Wuerth K, Hancock RE. Immune modulation by multifaceted cationic host defense (antimicrobial) peptides. Nat Chem Biol. 2013;9(12):761-8.
3. Mookherjee N, Anderson MA, Haagsman HP, Davidson DJ. Antimicrobial host defence peptides: functions and clinical potential. Nat Rev Drug Discov. 2020;19(5):311-32.
4. Bowdish DM, Davidson DJ, Scott MG, Hancock RE. Immunomodulatory activities of small host defense peptides. Antimicrob Agents Chemother. 2005;49(5):1727-32.
5. Zanetti M. Cathelicidins, multifunctional peptides of the innate immunity. J Leukoc Biol. 2004;75(1):39-48.
6. Durr UH, Sudheendra US, Ramamoorthy A. LL-37, the only human member of the cathelicidin family of antimicrobial peptides. Biochim Biophys Acta. 2006;1758(9):1408-25.
7. Overhage J, Campisano A, Bains M, Torfs EC, Rehm BH, Hancock RE. Human host defense peptide LL-37 prevents bacterial biofilm formation. Infect Immun. 2008;76(9):4176-82.
8. Seil M, Nagant C, Dehaye JP, Vandenbranden M, Lensink MF. Spotlight on Human LL-37, an Immunomodulatory Peptide with Promising Cell-Penetrating Properties. Pharmaceuticals. 2010;3(11):3435-60.
9. Tossi A, Sandri L, Giangaspero A. Amphipathic, alpha-helical antimicrobial peptides. Biopolymers. 2000;55(1):4-30.
10. Gronberg A, Mahlapuu M, Stahle M, Whately-Smith C, Rollman O. Treatment with LL-37 is safe and effective in enhancing healing of hard-to-heal venous leg ulcers: a randomized, placebo-controlled clinical trial. Wound Repair Regen. 2014;22(5):613-21.
11. De Y, Chen Q, Schmidt AP, Anderson GM, Wang JM, Wooters J, et al. LL-37, the neutrophil granule- and epithelial cell-derived cathelicidin, utilizes formyl peptide receptor-like 1 (FPRL1) as a receptor to chemoattract human peripheral blood neutrophils, monocytes, and T cells. J Exp Med. 2000;192(7):1069-74.
12. Scott MG, Davidson DJ, Gold MR, Bowdish D, Hancock REW. The human antimicrobial peptide LL-37 is a multifunctional modulator of innate immune responses. Journal of Immunology. 2002;169(7):3883-91.
13. van der Does AM, Beekhuizen H, Ravensbergen B, Vos T, Ottenhoff TH, van Dissel JT, et al. LL-37 directs macrophage differentiation toward macrophages with a proinflammatory signature. J Immunol. 2010;185(3):1442-9.
14. Davidson DJ, Currie AJ, Reid GSD, Bowdish DME, MacDonald KL, Ma RC, et al. The cationic antimicrobial peptide LL-37 modulates dendritic cell differentiation and dendritic cell-induced T cell polarization. Journal of Immunology. 2004;172(2):1146-56.
15. Alexandre-Ramos DS, Silva-Carvalho AE, Lacerda MG, Serejo TRT, Franco OL, Pereira RW, et al. LL-37 treatment on human peripheral blood mononuclear cells modulates immune response and promotes regulatory T-cells generation. Biomed Pharmacother. 2018;108:1584-90.
16. de Breij A, Riool M, Cordfunke RA, Malanovic N, de Boer L, Koning RI, et al. The antimicrobial peptide SAAP-148 combats drug-resistant bacteria and biofilms. Sci Transl Med. 2018;10(423).
17. Scheper H, Wubbolts JM, Verhagen JAM, de Visser AW, van der Wal RJP, Visser LG, et al. SAAP-148 Eradicates MRSA Persisters Within Mature Biofilm Models Simulating Prosthetic Joint Infection. Front Microbiol. 2021;12:625952.
18. Kaur N, Dilawari R, Kaur A, Sahni G, Rishi P. Recombinant expression, purification and PEGylation of Paneth cell peptide (cryptdin-2) with value added attributes against Staphylococcus aureus. Sci Rep. 2020;10(1):12164.
19. Imura Y, Nishida M, Matsuzaki K. Action mechanism of PEGylated magainin 2 analogue peptide. Biochim Biophys Acta. 2007;1768(10):2578-85.
20. Imura Y, Nishida M, Ogawa Y, Takakura Y, Matsuzaki K. Action mechanism of tachyplesin I and effects of PEGylation. Biochim Biophys Acta. 2007;1768(5):1160-9.
21. Guiotto A, Pozzobon M, Canevari M, Manganelli R, Scarin M, Veronese FM. PEGylation of the antimicrobial peptide nisin A: problems and perspectives. Farmaco. 2003;58(1):45-50.

22. Singh S, Papareddy P, Morgelin M, Schmidtchen A, Malmsten M. Effects of PEGylation on membrane and lipopolysaccharide interactions of host defense peptides. Biomacromolecules. 2014;15(4):1337-45.
23. Manteghi R, Pallagi E, Olajos G, Csoka I. Pegylation and formulation strategy of Anti-Microbial Peptide (AMP) according to the quality by design approach. Eur J Pharm Sci. 2020;144:105197.
24. Cui Q, Xu QJ, Liu L, Guan LL, Jiang XY, Inam M, et al. Preparation, Characterization and Pharmacokinetic Study of N-Terminal PEGylated D-Form Antimicrobial Peptide OM19r-8. J Pharm Sci. 2021;110(3):1111-9.
25. Morris CJ, Beck K, Fox MA, Ulaeto D, Clark GC, Gumbleton M. Pegylation of antimicrobial peptides maintains the active peptide conformation, model membrane interactions, and antimicrobial activity while improving lung tissue biocompatibility following airway delivery. Antimicrob Agents Chemother. 2012;56(6):3298-308.
26. Verreck FA, de Boer T, Langenberg DM, Hoeve MA, Kramer M, Vaisberg E, et al. Human IL-23-producing type 1 macrophages promote but IL-10-producing type 2 macrophages subvert immunity to (myco)bacteria. Proc Natl Acad Sci U S A. 2004;101(13):4560-5.
27. Geluk A, Van Meijgaarden KE, Janson AA, Drijfhout JW, Meloen RH, De Vries RR, et al. Functional analysis of DR17(DR3)-restricted mycobacterial T cell epitopes reveals DR17-binding motif and enables the design of allele-specific competitor peptides. J Immunol. 1992;149(9):2864-71.
28. Verreck FA, de Boer T, Langenberg DM, van der Zanden L, Ottenhoff TH. Phenotypic and functional profiling of human proinflammatory type-1 and anti-inflammatory type-2 macrophages in response to microbial antigens and IFN-gamma- and CD40L-mediated costimulation. J Leukoc Biol. 2006;79(2):285-93.
29. Nelson JW, Kallenbach NR. Stabilization of the ribonuclease S-peptide alpha-helix by trifluoroethanol. Proteins. 1986;1(3):211-7.
30. Wu CS, Yang JT. Sequence-dependent conformations of short polypeptides in a hydrophobic environment. Mol Cell Biochem. 1981;40(2):109-22.
31. Otzen DE, Sehgal P, Westh P. alpha-Lactalbumin is unfolded by all classes of surfactants but by different mechanisms. J Colloid Interf Sci. 2009;329(2):273-83.
32. Drayton M, Alford MA, Pletzer D, Haney EF, Machado Y, Luo HD, et al. Enzymatically releasable polyethylene glycol - host defense peptide conjugates with improved activity and biocompatibility. J Control Release. 2021;339:220-31.
33. Yu W, Wang J, Wang Z, Li L, Li W, Song J, et al. PEGylation of the Antimicrobial Peptide PG-1: A Link between Propensity for Nanostructuring and Capacity of the Antitrypsin Hydrolytic Ability. J Med Chem. 2021;64(14):10469-81.
34. Tjabringa GS, Ninaber DK, Drijfhout JW, Rabe KF, Hiemstra PS. Human cathelicidin LL-37 is a chemoattractant for eosinophils and neutrophils that acts via formyl-peptide receptors. Int Arch Allergy Imm. 2006;140(2):103-12.
35. Tomasinsig L, Pizzirani C, Skerlavaj B, Pellegatti P, Gulinelli S, Tossi A, et al. The human cathelicidin LL-37 modulates the activities of the P2X7 receptor in a structure-dependent manner. J Biol Chem. 2008;283(45):30471-81.
36. Xu Q, Keiderling TA. Effect of sodium dodecyl sulfate on folding and thermal stability of acid-denatured cytochrome c: a spectroscopic approach. Protein Sci. 2004;13(11):2949-59.
37. Veronese FM, Mero A. The impact of PEGylation on biological therapies. BioDrugs. 2008;22(5):315-29.
38. Dennison SR, Reddy SM, Morton LHG, Harris F, Badiani K, Phoenix DA. PEGylation enhances the antibacterial and therapeutic potential of amphibian host defence peptides. Biochim Biophys Acta Biomembr. 2022;1864(1):183806.
39. Cicchese JM, Evans S, Hult C, Joslyn LR, Wessler T, Millar JA, et al. Dynamic balance of pro- and anti-inflammatory signals controls disease and limits pathology. Immunol Rev. 2018;285(1):147-67.
40. Sica A, Schioppa T, Mantovani A, Allavena P. Tumour-associated macrophages are a distinct M2 polarised population promoting tumour progression: potential targets of anti-cancer therapy. Eur J Cancer. 2006;42(6):717-27.
41. Chen Y, Song Y, Du W, Gong L, Chang H, Zou Z. Tumor-associated macrophages: an accomplice in solid tumor progression. J Biomed Sci. 2019;26(1):78.
42. Etzerodt A, Tsalkitzi K, Maniecki M, Damsky W, Delfini M, Baudoin E, et al. Specific targeting of CD163(+) TAMs mobilizes inflammatory monocytes and promotes T cell-mediated tumor regression. J Exp Med. 2019;216(10):2394-411.